

RESEARCH

Open Access



NIEAs elicited by wild-type SARS-CoV-2 primary infection fail to enhance the infectivity of Omicron variants

Qi Gui^{1,2†}, Haiyan Wang^{2†}, Congcong Liu^{2†}, Wenting Li², Bing Zhou², Shilong Tang², Qing Fan², Xiangyang Ge², Bin Ju^{2,3*} and Zheng Zhang^{1,2,3,4*}

Abstract

SARS-CoV-2 infection widely induces antibody response targeting diverse viral proteins, including typical representative N-terminal domain (NTD), receptor-binding domain (RBD), and S2 subunit of spike. A lot of NTD-, RBD-, and S2-specific monoclonal antibodies (mAbs) have been isolated from COVID-19 convalescents, some of which displaying potent activities to inhibit viral infection. However, a small portion of NTD-specific mAbs elicited by wild-type (WT) SARS-CoV-2 primary infection could facilitate the virus entry into target cells in vitro, so called NTD-targeting infection-enhancing antibodies (NIEAs). To date, SARS-CoV-2 has evolved to massive variants carrying various NTD mutations, especially recent Omicron BA.2.86 and JN.1. In this study, we investigated whether these WT-NIEAs could still enhance the infectivity of emerging Omicron variants. Nine novel WT-NIEAs with diverse germline gene usage were identified from 3 individuals, effectively enlarging available antibody panel of NIEAs. Bivalent binding of NIEAs to inter-spike contributed to their infection-enhancing activities. WT-NIEAs could enhance the infectivity of SARS-CoV-2 variants emerged before Omicron, but ineffective to Omicron variants including BA.2.86 and JN.1, which was because of their changed antigenicity of NTDs. Overall, these data clearly demonstrated the cross-reactivity of these pre-existed WT-NIEAs to a series of SARS-CoV-2 variants, helping to evaluate the risk of enhanced infection of emerging variants in future.

[†]Qi Gui, Haiyan Wang and Congcong Liu contributed equally to this work.

*Correspondence:

Bin Ju

jubin2013@163.com

Zheng Zhang

zhangzheng1975@aliyun.com

Full list of author information is available at the end of the article

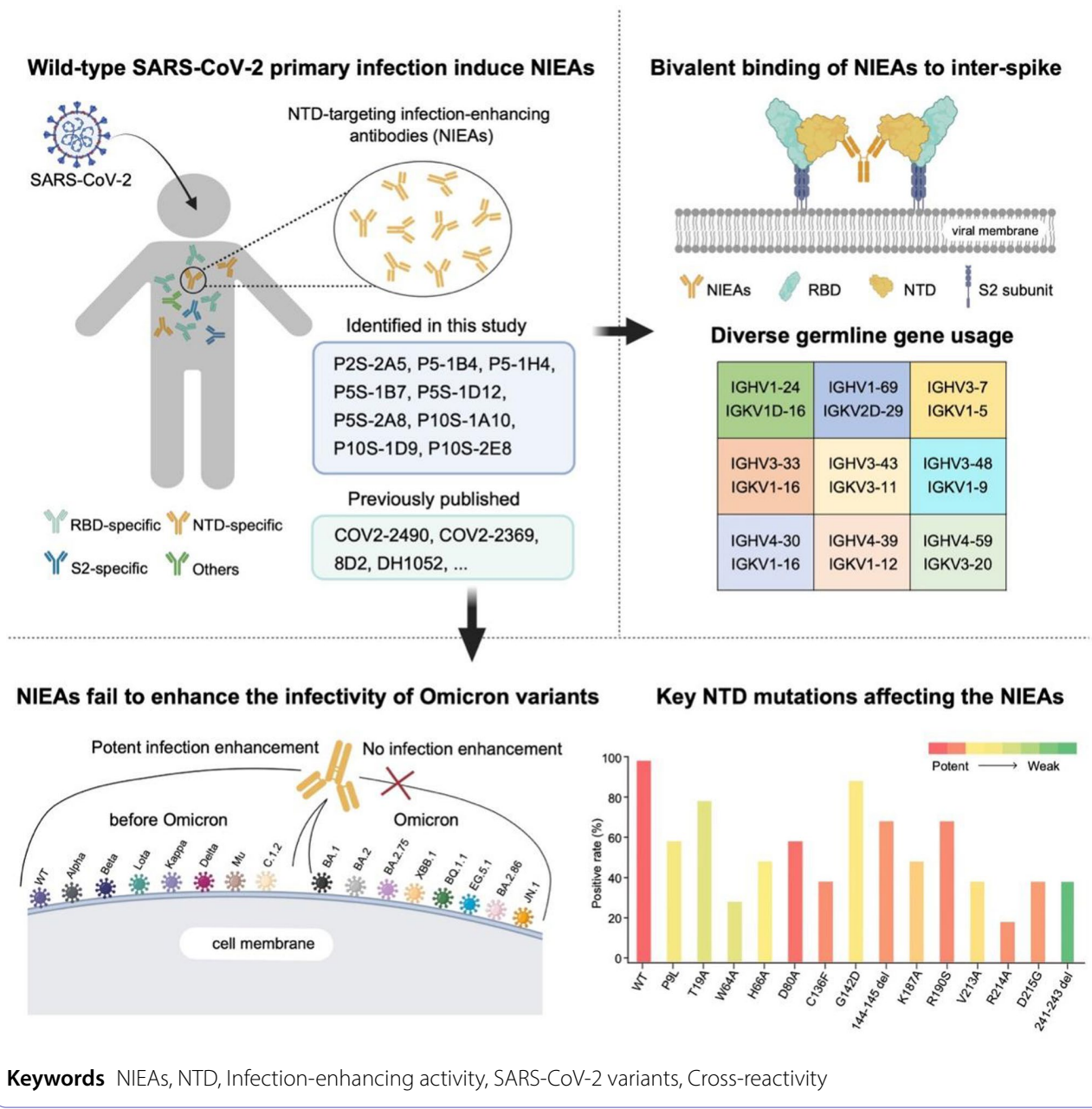


© The Author(s) 2025. **Open Access** This article is licensed under a Creative Commons Attribution-NonCommercial-NoDerivatives 4.0 International License, which permits any non-commercial use, sharing, distribution and reproduction in any medium or format, as long as you give appropriate credit to the original author(s) and the source, provide a link to the Creative Commons licence, and indicate if you modified the licensed material. You do not have permission under this licence to share adapted material derived from this article or parts of it. The images or other third party material in this article are included in the article's Creative Commons licence, unless indicated otherwise in a credit line to the material. If material is not included in the article's Creative Commons licence and your intended use is not permitted by statutory regulation or exceeds the permitted use, you will need to obtain permission directly from the copyright holder. To view a copy of this licence, visit <http://creativecommons.org/licenses/by-nc-nd/4.0/>.

Highlights

- Additional 9 NIEAs were identified from individuals infected with wild-type SARS-CoV-2.
- This Fc-independent enhancement was mediated by the divalent binding of F(ab)₂ to NTDs.
- NIEAs could not enhance the infectivity of Omicron variants including BA.2.86 and JN.1.
- Changed antigenicity of Omicron variants led to the ineffectiveness of WT-induced NIEAs.

Graphical abstract



Introduction

Highly pathogenic human coronaviruses (CoV) have recurrently instigated substantial global public health emergencies. The outbreak of Severe Acute Respiratory Syndrome Coronavirus (SARS-CoV) in 2003, the

emergence of Middle East Respiratory Syndrome Coronavirus (MERS-CoV) in 2012, and the ongoing global pandemic of Severe Acute Respiratory Syndrome Coronavirus 2 (SARS-CoV-2) since the end of 2019 have all exerted a significant threat to the global economy and

public health [1–6]. The speed of spread and infectivity of SARS-CoV-2 exceeded those of SARS-CoV and MERS-CoV, with a wider range of organ involvement, including heart, kidneys, and gastrointestinal tract [7–9]. A furin cleavage site at the S1/S2 boundary of the SARS-CoV-2 spike protein was a novel feature relative to SARS-CoV that may exhibit higher affinity to the host cell receptor angiotensin-converting enzyme-2 (ACE2), which contributed to the global pandemic [10, 11]. SARS-CoV-2 is a type of enveloped RNA virus with a single positive-strand genome, primarily composed of 4 structural proteins: nucleocapsid protein (N), membrane protein (M), envelope protein (E), and spike protein (S) [12]. The spike protein is the crucial structural protein, playing a pivotal role in mediating viral infection into host cells [12]. Functionally, the spike protein is divided into S1 and S2 subunits [13]. S1 subunit primarily facilitates the virus binding to human ACE2 and S2 subunit is crucial for the fusion of the virus with the host cell membrane [13–15]. The S1 subunit is comprised of the receptor-binding domain (RBD), the N-terminal domain (NTD), as well as subdomains SD1 and SD2 [12]. Antibodies targeting RBD, such as SA55, can prevent the virus to entry host cells by disrupting the interaction between the virus and the host cell ACE2 receptor [16]. Antibodies targeting NTD also can interfere with the virus-receptor binding process in different ways [17–20]. For example, BLN12 can inhibit the interaction of the NTD with C-type lectin receptors, thereby inhibiting SARS-CoV-2 infection [17]. 4A8 can enhance the “wedge” effect of the NTD, locking the RBD in a downward conformation and preventing the conformational change of the spike protein [19, 20]. The neutralization mechanism of C1717 may prevent viral entry into host cells by inducing the shedding of S1 subunit [18]. Additionally, some antibodies targeting S2 subunit, like 76E1 [21], can also destroy SARS-CoV-2 infection by inhibiting the viral membrane fusion process [22, 23]. Currently, research mainly focuses on RBD-, NTD-, and S2-specific neutralizing antibodies [17–19, 24, 25]. In addition to neutralizing effects, some antibodies can also promote viral infection to host cells [19, 26–29]. For instance, some antibodies recognizing the NTD can markedly enhance viral infection, including COV2-2490, COV2-2369, 8D2, and DH1052 [19, 27, 28]. These antibodies are referred to as NTD-targeting infection-enhancing antibodies (NIEAs) [26, 29, 30]. These NIEAs reported in previous studies targeted similar epitopes on the NTD, which enhanced the binding of spike protein to ACE2 and promoted infection through the same mechanism [26, 28–30]. Liu et al. found a model of two inter-spike proteins bound with a single divalent enhancing antibody, which was required to induce the RBD-up state [26]. Tina Lusiany et al. further provided a direct evidence confirming the spike-NIEA-spike crosslinking

model [30]. Another studies of NIEAs utilizing respiratory (Calu-3) and intestinal (Caco-2) epithelial cell lines in the infection enhancement experiment, which expressed lower levels of ACE2, demonstrated that this kind of antibody-mediated infection enhancement was related to the expression level of the ACE2 receptor on target cells [29]. SARS-CoV-2 continues to mutate, however, current research on NIEAs is limited to their infection-enhancing effects on the original strain. Omicron variants have contained numerous mutations, yet it remains unclear whether these NIEAs could still enhance the infectivity of heavily mutated variants.

In May 2023, the World Health Organization (WHO) declared that the COVID-19 pandemic no longer constitutes a public health emergency of international concern. However, the continued evolution of SARS-CoV-2 variants has presented a constant challenge toward protection and host immunity, giving rise to the emergence of various variants that spread globally [31, 32]. Some of the most well-known variants include Alpha, Delta, and subvariants of the Omicron lineage such as BA.1, BA.2, BA.2.86, and JN.1. The Alpha variant, which emerged as the first variant of concern (VOC) in September 2020, contained a key mutation at residue N501 [33]. This alteration resulted in an increased affinity for the variant to bind to the ACE2 receptor, potentially enhancing the transmissibility of the variant [33]. In late 2020, the Delta variant was first identified in the state of Maharashtra. Compared to previously existing variants, the Delta variant exhibited significantly higher transmission rates. Mutations present in the Delta variant, such as L452R and T478K, facilitated the increased infectivity and immune evasion [32, 34]. The Omicron variants belong to a family of strains that emerged in late 2021, several subvariants of which have rapidly evolved. BA.1, the first Omicron subvariant, had 33 mutations within the spike protein, including mutations at K417, E484, and N501. These mutations led to BA.1 to partially evade immunity from previous infections and vaccinations [35]. As of March 2022, Omicron BA.2 surpassed BA.1 as the dominant subvariant. BA.2 shared many mutations with BA.1, but had some differences in the spike protein, such as T376A, D405N, and R408S. More mutations may lead to higher pathogenic potential and further immune escapes [36–38]. BA.2.86 and JN.1 were two Omicron subvariants that emerged with a different mutation profile, also carrying multiple mutations in the spike protein and displaying increased antibody evasion [31, 39, 40]. Compared to BA.2.86, JN.1 carried the L455S substitution, that may affect its ability to bind to the ACE2 receptor and potentially reduce the effectiveness of monoclonal antibodies (mAbs) [41, 42]. According to the present research, these SARS-CoV-2 variants have evaded the neutralization of plasma from convalescent individuals

and those who have been vaccinated [43–45]. Previously, the research has described the infection-enhancing activity of NIEAs against the wild-type (WT) SARS-CoV-2, yet it is not clear whether these mAbs still have enhancement effect against Omicron subvariants.

In this study, we identified 9 novel NIEAs from three COVID-19 convalescents infected with WT SARS-CoV-2. This kind of infection-enhancing activity is dependent on the bivalent binding to inter-spike NTDs, rather than interactions mediated by the Fc region. Genetic analysis revealed that these 9 NIEAs originated from distinct germline genes, reflecting the complexity of antibody response. These 9 NIEAs could not enhance the infectivity of Omicron variants including BA.2.86 and JN.1, indicating that changed sequences of variants affected the infection-enhancing activities of NIEAs. Finally, we mapped the specific binding sites of these 9 NIEAs to explore the altered antigenicity of Omicron variants and identified that certain mutations, such as

P9L, T19A, and D80A, may not impact the infection-enhancing activities of NIEAs against subsequently emerging variants. These results expanded the antibody panel of NIEAs and enriched the understanding of antibodies enhancing viral infectivity.

Results

Nine NTD-targeting infection-enhancing antibodies elicited by WT SARS-CoV-2 infection

Previously, we isolated a series of SARS-CoV-2 spike-specific mAbs from individuals who had recovered from wild-type SARS-CoV-2 infection, 130 of which bound to neither RBD nor S2 of spike [46]. After screening for their abilities to inhibit the virus entry, we found 9 non-neutralizing mAbs from three individuals (P2, P5, and P10) could obviously enhance the SARS-CoV-2 pseudovirus to infect HEK293T-hACE2 cells, which were named as P2S-2A5, P5-1B4, P5-1H4, P5S-1B7, P5S-1D12, P5S-2A8, P10S-1A10, P10S-1D9, and P10S-2E8 (Fig. 1a).

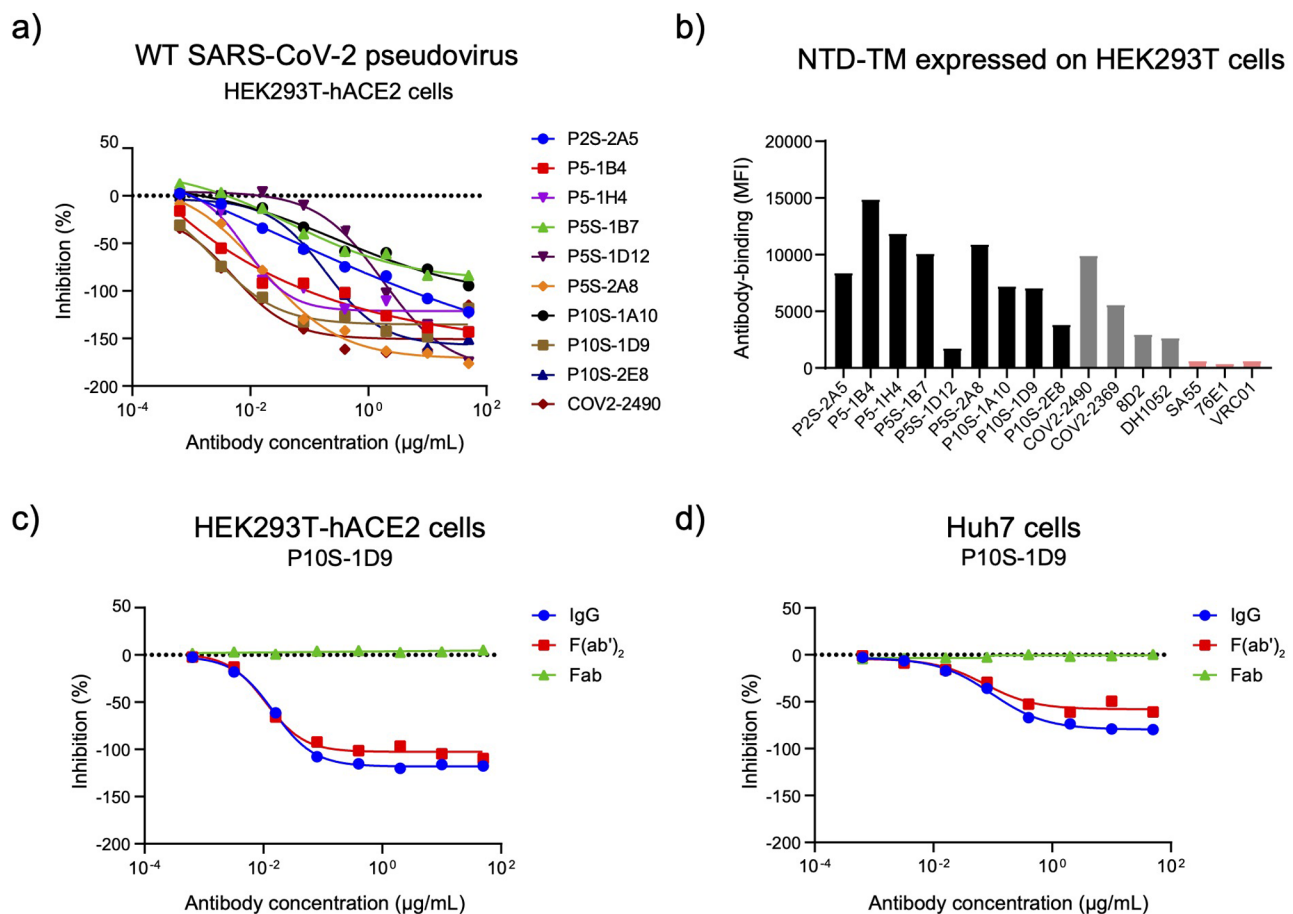


Fig. 1 Enhancement activity and binding capacity of 9 NTD-targeting infection-enhancing antibodies (NIEAs). The infection-enhancing activity (a) and binding capacity (b) of P2S-2A5, P5-1B4, P5S-1B7, P5-1H4, P5S-2A8, P10S-1A10, P10S-1D9, P10S-2E8, and P5S-1D12 were measured by the pseudovirus infection assay and flow cytometry analysis. COV2-2490, COV2-2369, 8D2, and DH1052 were published NIEAs as positive controls. SA55 (anti-SARS-CoV-2 RBD), 76E1 (anti-SARS-CoV-2 S2), and VRC01 (anti-HIV-1) were non-NIEAs as negative controls. The infection-enhancing activity of IgG-, F(ab)₂- and Fab-form P10S-1D9 were measured using HEK293T-hACE2 cells (c) and Huh7 cells (d). The experiments were performed twice and one representative result was shown

P5S-2A8 exhibited the most potent infection-enhancing activity, while P5S-1B7 showed a comparatively weaker enhancement effect. To further determine the binding region of these 9 infection-enhancing mAbs, we expressed the NTD of spike on the HEK293T cell membrane through coupling with a transmembrane domain and then detected their binding capacities by 9 mAbs. As shown in Fig. 1b and S1, all 9 mAbs were able to bind to the NTD of SARS-CoV-2 spike by the flow cytometry analysis. These results indicated that we identified 9 infection-enhancing mAbs specifically targeting the NTD region of SARS-CoV-2 spike, usually called NTD-targeting infection-enhancing antibodies (NIEAs) [30].

A postulated mechanism of NIEAs is based on their dual attachment to the NTD, which is located adjacent to the RBD. This divalent interaction triggers a conformational change of RBD, thus enhancing an enhanced ability of RBD to recognize ACE2 receptors. This process is independent on the interaction between Fc domain and Fc γ receptors [26]. In this study, as a representative of NIEAs, IgG-form P10S-1D9 was digested to different antibody fragments: F(ab')₂ and Fab. All full-length IgG-, F(ab')₂-, and Fab-form P10S-1D9 could effectively bind to the SARS-CoV-2 spike trimer protein (Fig. S2). Consistent with previous studies [29, 30], both bivalent IgG and F(ab')₂ fragments of P10S-1D9 obviously enhanced the infectivity of SARS-CoV-2 to HEK293T-hACE2 cells with similar potency, but monovalent P10S-1D9 Fab did not (Fig. 1c). Meanwhile, Huh7 cells expressing lower level of hACE2 receptors than HEK293T-hACE2 cells were also used as the targeted cells to detect the infection-enhancing activities of IgG- and F(ab')₂-form P10S-1D9. As shown in Fig. 1d, P10S-1D9 displayed slightly lower infection-enhancing activity than that tested in HEK293T-hACE2 cells. These results confirmed that bivalent antibody binding to the NTD was required for the enhancement of SARS-CoV-2 infection in vitro, rather than interactions mediated by antibody Fc region with Fc γ receptor on downstream effector cells.

Varied affinities of 9 NIEAs binding to soluble NTD proteins

To measure the binding capacity of 9 NIEAs, we first constructed, expressed, and purified soluble WT SARS-CoV-2 spike trimer and NTD proteins (Fig. S3a). All 9 NIEAs identified here and 4 control NIEAs reported in previous studies [19, 27, 28] could strongly bind to the spike trimer, however, P2S-2A5, P10S-2E8, P5S-1D12, 8D2, and DH1052 exhibited weak or no binding ability to the NTD monomer protein by ELISA (Figs. S3b and c). To quantify the binding affinity of these 9 NIEAs, we further performed the SPR analysis. As shown in Fig. 2, P5-1B4, P5S-1B7, P5-1H4, P5S-2A8, P10S-1A10, and P10S-1D9 displayed strong binding affinities to NTD in a nanomolar range from 0.554 nM to 9.415 nM, P2S-2A5

showed a relatively weak affinity with the K_D value of 182 nM, yet P10S-2E8 and P5S-1D12 did not bind to soluble NTD proteins by SPR. Collectively, NIEAs exhibited different binding patterns and potencies to cell-surface-expressed NTD (Fig. 1b), soluble spike trimer (Fig. S3b), and soluble NTD proteins (Fig. 2), suggesting that NIEAs might have diverse recognition features in the antibody-antigen interface.

Genetic analysis of 9 NIEAs

The program IMGT/V-QUEST (www.imgt.org/IMGT_vquest) was used to analyze variable genes of 9 NIEAs identified here and 4 control NIEAs reported in previous studies [19, 27, 28]. As shown in Table 1, heavy chains of these NIEAs were derived from multiple germline genes including IGHV1-24, IGHV1-69, IGHV3-7, IGHV3-30, IGHV3-33, IGHV3-43, IGHV3-48, IGHV4-30, IGHV4-39, and IGHV4-59. Although DH1052 and P10S-1A10 shared IGHV1-69 and 8D2, COV2-2490, and P5-1H4 all belonged to IGHV3-7, their complementarity determining region 3 (CDR3) loops were markedly different in the amino acid sequence. Interestingly, all light chains of 13 NIEAs were derived from the kappa germline gene, yet none of them utilized the lambda germline gene. In general, the somatic hypermutations (SHMs) of both heavy and light chains were relatively low. These results demonstrated that the public clone phenomenon was not common in SARS-CoV-2 NIEAs, reflecting the complexity and diversity of human antibody response.

Cross-reactivity of 9 NIEAs to a series of SARS-CoV-2 variants

Mutations in the NTD have altered its immunogenicity, contributing to the emergence of more adaptive and invasive variants [47–49]. To evaluate the cross-reactivity of these 9 NIEAs elicited by WT SARS-CoV-2 primary infection to subsequent variants, we prepared 15 pseudovirus variants including Alpha, Beta, Lota, Kappa, Delta, Mu, and C.1.2, as well as Omicron BA.1, BA.2, BA.2.75, XBB.1, BQ.1.1, EG.5.1, BA.2.86, and JN.1, and measured their sensitivities to 9 NIEAs identified in this study and a control NIEA named COV2-2490. As shown in Fig. 3a and S4, before the emerging of Omicron variants, the infectivity of SARS-CoV-2 variants except Beta and C.1.2 were obviously enhanced by most of NIEAs. Wherein Kappa and Delta variants were especially sensitive to these NIEAs, whose maximum enhancements could easily reach more than 150% at the low concentration. With the emerging of Omicron variants including recent BA.2.86 and JN.1, these NIEAs failed to enhance the infection of Omicron variants to targeted HEK293T-hACE2 cells.

To investigate the potential mechanism underlying the loss of infection-enhancing abilities of these NIEAs

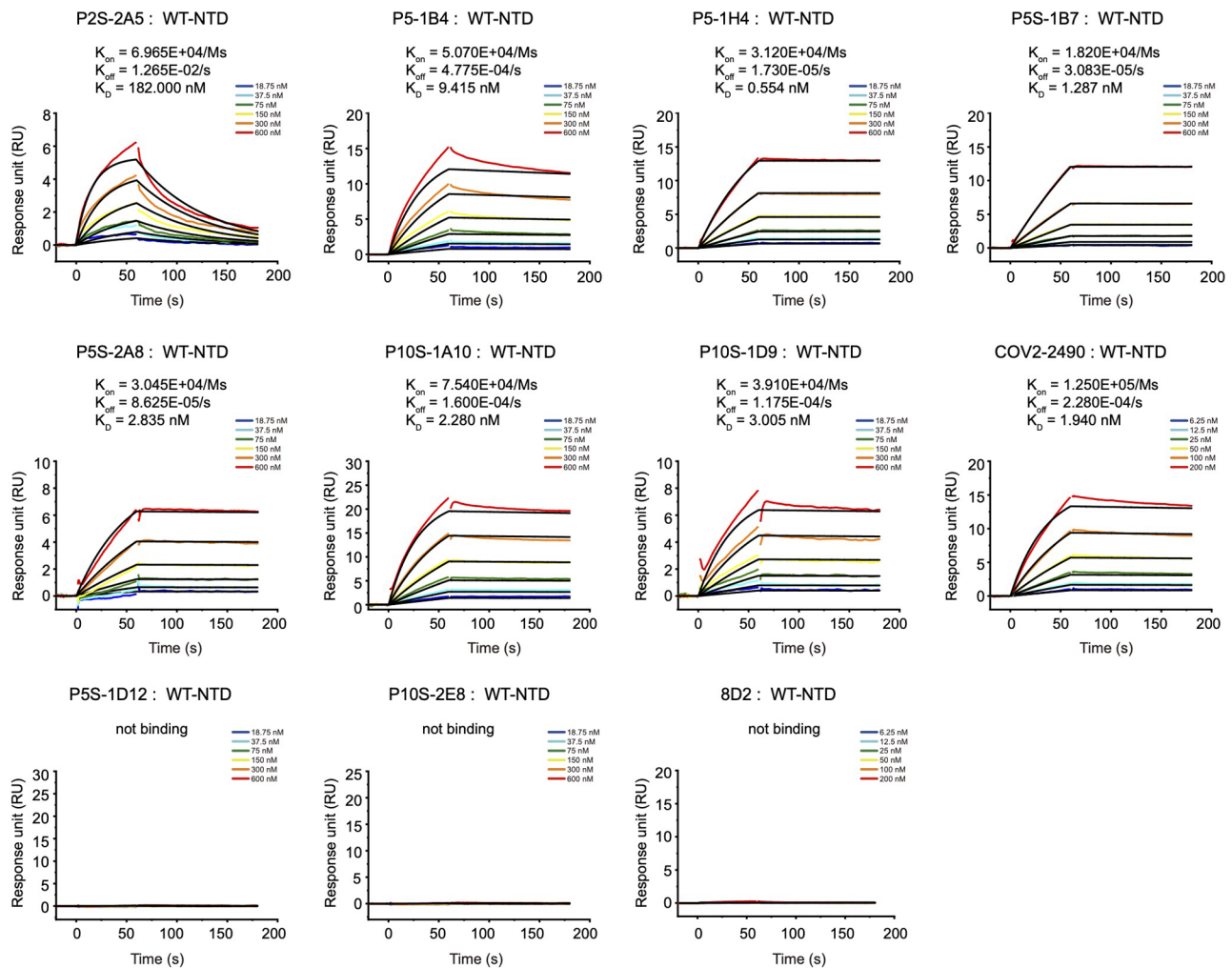


Fig. 2 Binding affinities of NIEAs to soluble WT SARS-CoV-2 NTD proteins by SPR. The association rate constant (K_{on}), dissociation rate constant (K_{off}), and dissociation constant (K_D) were calculated from three independent experiments and represented in mean values. One representative curve was shown

against Omicron variants, we performed ELISA and flow cytometry assay to evaluate their binding capacities to spike proteins of Omicron variants. We selected BA.1 and BA.2.86 variants as the representative, possessing more special mutations compared with other variants. As shown in Fig. S5a, the binding capacities of these NIEAs to BA.1 and BA.2.86 soluble spike proteins were almost completely lost. To exclude the possibility that the loss of binding capacity was due to the conformational change of soluble proteins, we further used flow cytometry to measure the binding capacities of these NIEAs to membrane-expressed BA.1 and BA.2.86 spike proteins (Fig. S5b). The results were consistent with the ELISA experiment, showing that these NIEAs hardly bound to the BA.1 and BA.2.86 spike proteins. To exclude the potential effect of transient transfection efficiency, we further constructed the stable HEK293T cell line expressing BA.1 spike protein and measured their binding capacities by NIEAs. All results showed that these NIEAs could not bind to the

heavily mutated BA.1 and BA.2.86 spike proteins. These findings suggested that the loss of infection-enhancing activity of NIEAs against Omicron variants should be due to their inability of binding to the spike proteins of these variants.

Key amino acid residues affecting the recognition of NIEAs

Determining the antibody recognition sites is crucial for understanding the mechanism of NIEAs enhancing the virus infection. Previous studies have demonstrated that NIEAs mainly target analogous epitopes located on the exterior of NTD [26, 29, 30]. To identify the binding epitopes of these 9 NIEAs, we first performed a competition ELISA to test their competitively binding to the WT SARS-CoV-2 spike trimer with 8D2, a representative NIEA with well-known structural information [26]. Eight of NIEAs exhibited an obvious competition of more than 50% with 8D2, however, P5S-1D12 displayed a markedly lower competition level at 22.10% (Figs. S6a and b). Then, we labeled

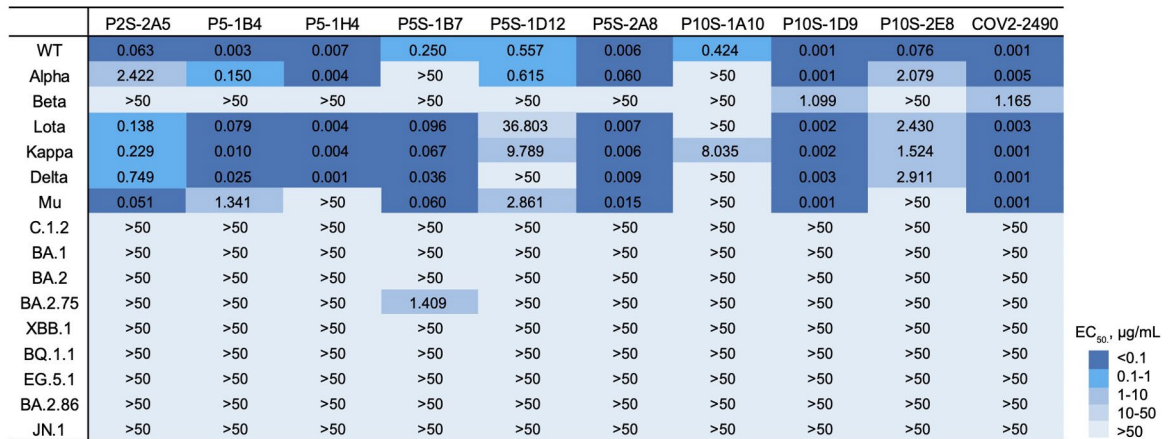
Table 1 Gene family analysis of NTD-targeting infection-enhancing antibodies

mAbs	Heavy chain						Light chain				
	V _H Gene	D _H Gene	J _H Gene	CDR3 (amino acids)	CDR3 length	% SHM	V _L Gene	J _L Gene	CDR3 (amino acids)	CDR3 length	% SHM
P5S-1D12	IGHV1-24	IGHD3-3	IGHJ2	ATGSGYSSHWNWYFDL	16	0	IGKV1D-16	IGKJ4	QQYNSYPLT	9	0
DH1052*	IGHV1-69	IGHD2-21	IGHJ4	ATSSGSPRLCGGGSCYHSFDY	21	0	IGKV3-20	IGKJ1	QQYGSPTWT	10	0
P10S-1A10	IGHV1-69	IGHD2-15	IGHJ6	AREGVVAATPLYGMDV	18	0.7	IGKV2D-29	IGKJ2	MQSIHLPYT	9	0.7
8D2*	IGHV3-7	IGHD3-9	IGHJ3	ARDWDYDILTSWFGAFDI	19	1.4	IGKV1-17	IGKJ4	LQHNSYPLT	9	0
COV2-2490*	IGHV3-7	IGHD3-3	IGHJ4	ARDPYDLYGDYGGTFDY	17	2.7	IGKV1-5	IGKJ4	QQYNSYSLT	9	1.1
P5-1H4	IGHV3-7	IGHD2-15	IGHJ4	ARDLTEAYCSGGGCSEGFY	20	2.8	IGKV1-5	IGKJ2	QQYHSYPVT	9	1.8
COV2-2369*	IGHV3-30	IGHD5-18	IGHJ4	AKDFGGDNTAMVEYFFDF	18	2.4	IGKV1-5	IGKJ1	QQYNSYSPT	9	0
P5-1B4	IGHV3-33	IGHD4-17	IGHJ4	AKDFGNDYGDIGGNFDY	17	2.4	IGKV1-16	IGKJ4	QQYHSYPLT	9	0.7
P10S-1D9	IGHV3-43	IGHD3-10	IGHJ6	AKDLGSYNYGYGMDV	15	1.7	IGKV3-11	IGKJ4	QQRSNWPLT	9	0
P10S-2E8	IGHV3-48	IGHD3-22	IGHJ5	ARDFSNYYDSSGYVFN-WFDP	22	0.3	IGKV1-9	IGKJ4	QLLNSYPPT	9	0
P5S-2A8	IGHV4-30	IGHD3-22	IGHJ4	ARGHYSYDNSGTFDY	15	2.1	IGKV1-17	IGKJ4	LQHNTYPLT	9	0.7
P2S-2A5	IGHV4-39	IGHD2-15	IGHJ6	ARDRDSAGSRIMGGMDV	17	0.3	IGKV1-12	IGKJ3	QQANSFPPT	9	0
P5S-1B7	IGHV4-59	IGHD2-15	IGHJ4	AKGDVESCSCYDF	18	2.8	IGKV3-20	IGKJ3	QHYGGSPLFT	10	2.5

*Previously published NTD-targeting infection-enhancing antibodies

The program IMGTV-QUEST was applied to analyze the gene germline, complementarity determining region 3 (CDR3), and somatic hypermutation (SHM). The SHM frequency was calculated from the mutated nucleotides

a)



b)

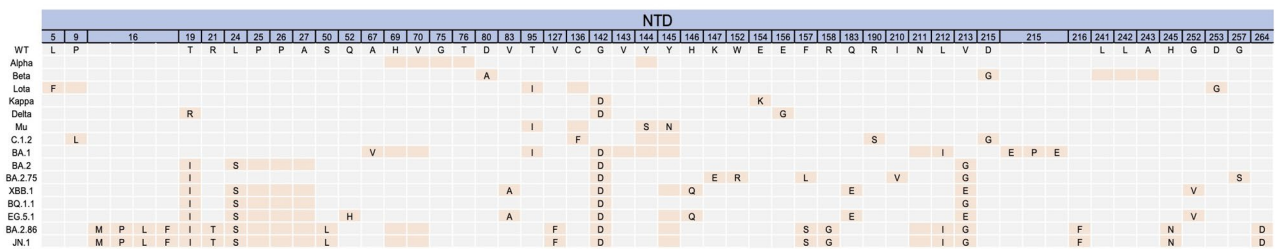


Fig. 3 The susceptibility and sequence alignment of SARS-CoV-2 variants to NIEAs. **(a)** Cross-reactivity of NIEAs to a series of SARS-CoV-2 variants including Alpha, Beta, Lota, Kappa, Delta, Mu, and C.1.2, as well as Omicron BA.1, BA.2, BA.2.75, XBB.1, BQ.1.1, EG.5.1, BA.2.86, and JN.1. Experiments were performed twice and data were shown in mean values. **(b)** Amino acid sequence alignment of NTDs from all tested SARS-CoV-2 pseudoviruses

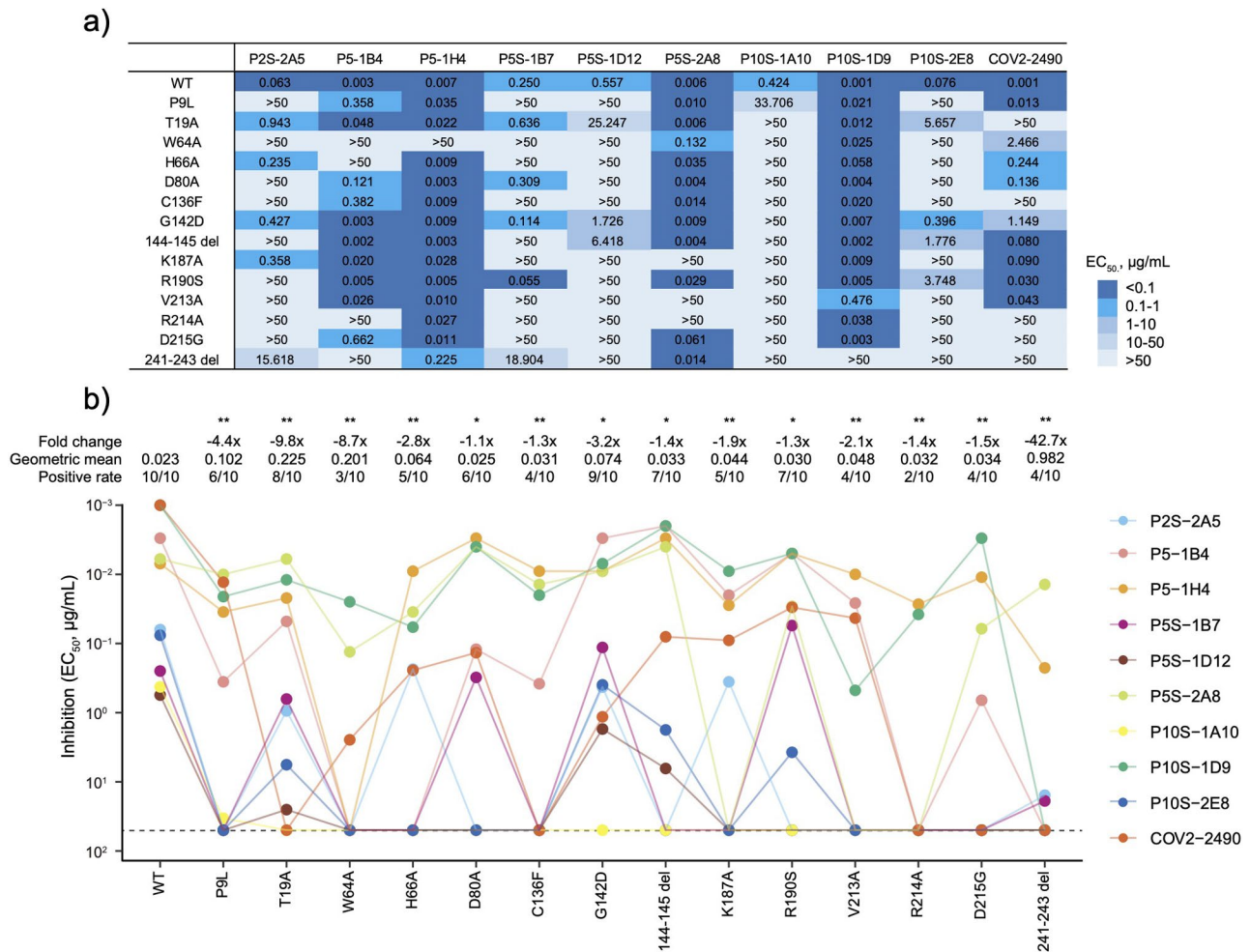


Fig. 4 Identification of binding epitopes of NIEAs. **(a)** The infection-enhancing activity of NIEAs to a series of SARS-CoV-2 single-point mutated pseudoviruses. Experiments were performed twice and data were shown in mean values. **(b)** These infection-enhancing results were shown by different mutations and compared with that against WT. The positive rate, geometric mean EC_{50} , fold change, and significance of difference were labeled on the top. “-” represented decreased the infection-enhancing activity. The statistical significance was performed using two-tailed paired Wilcoxon test. ** $p < 0.01$; * $p < 0.05$

P5S-1D12 with HRP and performed the competition ELISA again. All tested NIEAs including 4 control NIEAs strongly competed with P5S-1D12 (Figs. S6a and c). These results suggested that SARS-CoV-2 infection-enhancing antibodies recognized overlapping epitopes present on the NTD.

To further determine the key amino acid residues significantly affecting the recognition of NIEAs, we constructed a series of single-point mutated pseudoviruses based on the WT SARS-CoV-2 and measured their susceptibilities to a panel of 10 NIEAs including P2S-2A5, P5-1B4, P5-1H4, P5S-1B7, P5S-1D12, P5S-2A8, P10S-1A10, P10S-1D9, P10S-2E8, and COV2-2490. As shown in Fig. 4a and S7, all tested substitutions and deletion mutations affected the infection-enhancing activities of these NIEAs, more or less. To better quantitatively analyze these effects, we adjusted these infection-enhancing results by different mutations to compare them with that against WT (Fig. 4b). More than 50% of NIEAs

maintained the infection-enhancing activities against viruses carrying P9L, T19A, D80A, G142D, 144–145 del, and R190S, to a certain degree. By contrast, the mutations appearing on the position of 64, 66, 136, 187, 213, 214, 215, and 241 to 243 would lead to most of these NIEAs losing their infection-enhancing activities. These results indicated that NIEAs elicited by the WT SARS-CoV-2 primary infection could still enhance the infectivity of subsequently emerging variants even with some mutations, such as P9L, T19A, and D80A etc.

To further analyze how these mutations affect the binding and function of NIEAs, structural analysis were performed based on the available atomic models of the three NIEAs: DH1052 (PDB: 7LAB), 8D2 (PDB: 7DZX), and COV2-2490 (PDB: 7DZY). Unlike the neutralizing antibodies, whose epitopes face the host cell, all these three epitopes for NIEAs bind to the spike protein in a similar manner, facing the viral membrane [26, 29, 30] (Fig. 5a).

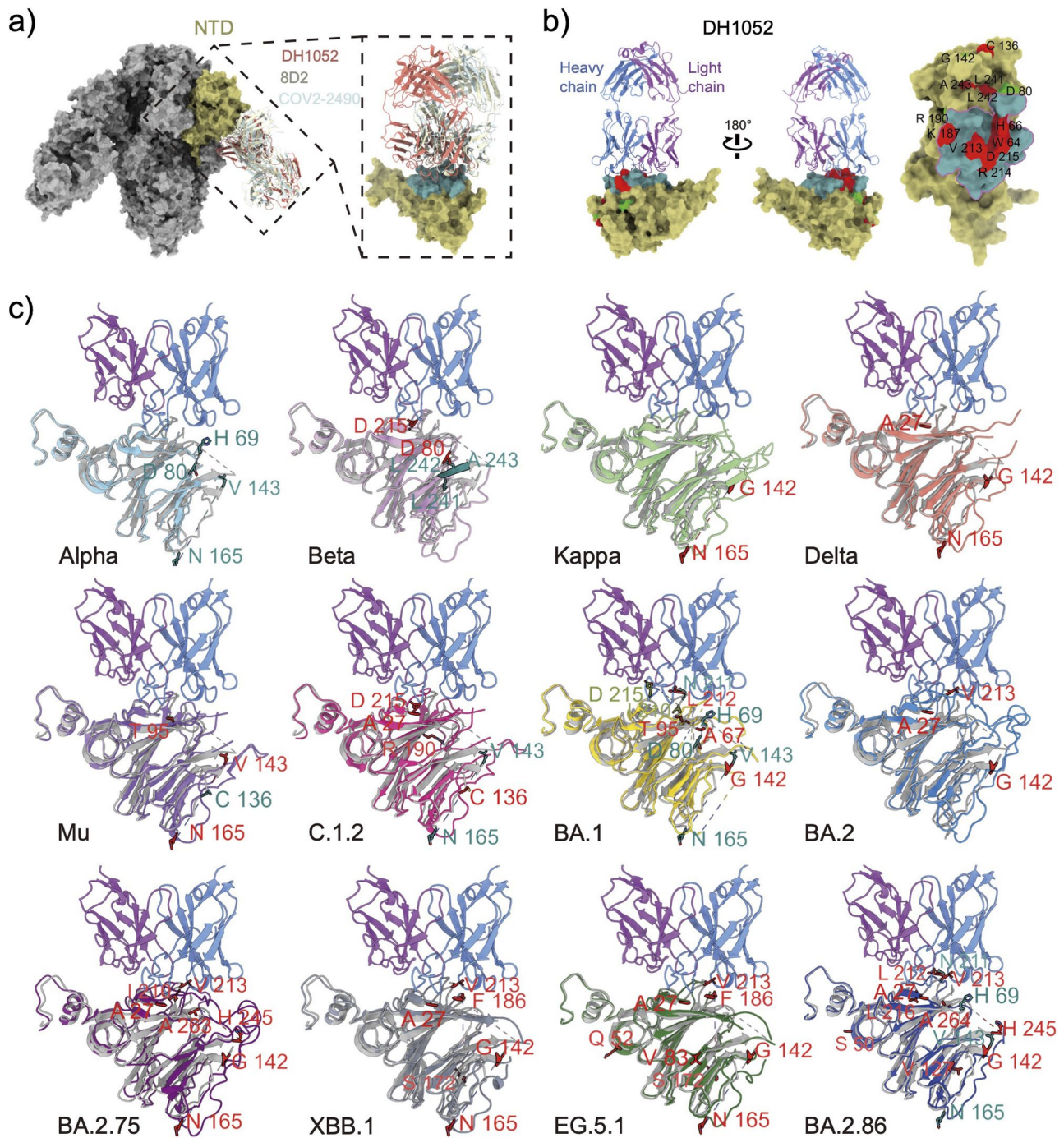


Fig. 5 Structures of NIEAs bound to the NTD protein of SARS-CoV-2 variants. **(a)** The epitopes of NIEAs, namely DH1052 (PDB: 7LAB), 8D2 (PDB: 7DZX), and COV2-2490 (PDB: 2DZY) face the viral membrane. NIEAs are shown as cartoon, and colored orange, light goldenrod yellow, and light cyan, respectively. The other parts are shown as surface. The related NTD of NIEAs is colored yellow. **(b)** Footprint of DH1052 on spike NTD. The light chain and heavy chain of DH1052 are colored orchid and blue. The footprint is colored cadet blue and circled out by violet red line. Sites that affect and those that do not affect antibody-mediated enhancement of infection are colored red and green, respectively. **(c)** Mutation sites of 12 different SARS-CoV-2 variants are mapped onto the NTDs. The accession numbers for the NTD atomic model in PDB are 7R14 (Alpha), 7R16 (Beta), 7VXC (Kappa), 8HRI (Delta), 7YBJ (Mu), 7YBM (C.1.2), 8HHZ (BA.1), 7XIW (BA.2), 7YQT (BA.2.75), 8IOS (XBB.1), 8XMT (EG.5.1) and 8XLV (BA.2.86). The key amino acids are shown as sticks. Mutated amino acids are colored red, inserted amino acids are colored olive drab, and deleted amino acids are colored teal. The amino acids at both ends of the key amino acid sites that are missing in the atomic model of DH1052 are marked. The structure figures were prepared using ChimeraX (<http://www.cgl.ucsf.edu/chimera>)

Meanwhile, the results of the competition of NIEAs binding to the WT SARS-CoV-2 spike trimer showed that all 9 NIEAs identified in our study shared similar epitopes with DH1052, 8D2, and COV2-2490 (Fig. S6). Since the atomic model of DH1052 is relatively complete, it is selected as the typical structure of these NIEAs for epitope analysis (Fig. 5b). Single-point mutation experiments had shown that most of the epitopes for the NIEAs in this study were concentrated in the footprint of DH1052 on NTD. Sites 64, 66, 187, 213, 214, and 215, which affect antibody-mediated enhancement of infection, are located in this area. In contrast, sites 9, 19, 80, 142, 144-145del, and 190, which are likely not to affect antibody activity, are found outside this region. Additionally, the mutations on the NTDs of 12 different SARS-CoV-2 variants were mapped onto the atomic models (Fig. 5c), and it was found that the Beta, C.1.2, and Omicron variants, which led to the loss of the enhancing effect of most NIEAs, shared a common mutation region, 213–215. These findings suggested that the 213–215 region may be the key site influencing antibody-mediated enhancement of infection.

Discussion

The NTD is a crucial structural component of the SARS-CoV-2 spike protein, playing a significant role in the virus entry into host cells [19, 26–30]. Therefore, antibodies targeting NTD might have some impact on the process of SARS-CoV-2 entry, displaying two quite different characteristics: neutralizing antibodies (nAbs) and infection-enhancing antibodies (NIEAs).

The infection enhancement mediated by NIEAs is different from traditional ADE, which was first reported in 1990 from a study on feline infectious peritonitis virus (FIPV) [50]. It is a safety concern for vaccine and antibody clinical use. It has been reported in several viruses, such as dengue virus, respiratory syncytial virus, MERS-CoV, and SARS-CoV [51–54]. In previous studies, the mechanism was dependent on the Fc receptor, since virus bound by antibodies could be absorbed by immune cells such as monocytes, macrophages, and B cells [55]. The mechanism of infection enhancement mediated by NIEAs has been widely reported as independent of Fc receptor (FcR) engagement [26, 29, 30]. Moreover, HEK293T-hACE2 target cells used in this experiment lack the expression of FcR, directly demonstrating the FcR-independent infection enhancing mechanism. This kind of infection enhancement was not the first report in this study [26, 29, 30]. Liu et al. previously discovered a non-canonical Fc-receptor-independent ADE mechanism of NIEAs [26]. Here, we further confirmed that this kind of NIEAs exerted their enhancement effect independent of the Fc receptor, distinguishing them from the traditional ADE. To validate this, a randomly selected

antibody was used as a representative to assess its Fc functional characteristics. Moreover, according to the previous research, NIEAs did not enhance SARS-CoV-2 infection in mouse or macaque models, indicating that NIEAs might not have ADE *in vivo* [26, 29, 30, 56]. These NIEAs might possess other Fc receptor-mediated effector functions, such as antibody-dependent cell-mediated cytotoxicity (ADCC), antibody-dependent cellular phagocytosis (ADCP), and etc.

Several NIEAs against SARS-CoV-2 were identified in previous research including COV2-2490, COV2-2369, 8D2, and DH1052 [19, 27, 28]. The cryo-EM structure of NIEAs were also obtained. Compared to the published mAbs, 9 NIEAs isolated in this study also exhibited an infection-enhancing effect to SARS-CoV-2 by bivalently binding to the NTD of the spike protein, and this enhancement was correlated with the expression level of ACE2 on target cell membrane. Similar to 8D2 with a published structure, some NIEAs in this study, such as P5S-1D12, could not bind to the soluble recombinant NTD protein but weakly recognize NTD protein expressed on the cell surface. This might be due to the differences in their antigenicity [19, 26–28].

In previous studies, the infection-enhancing effects of NIEAs were primarily tested against WT, BA.1, or BA.2 variants [26, 29]. However, we performed a more comprehensive analysis of NIEAs affecting the infectivity of WT SARS-CoV-2 and a series of variants, including Alpha, Beta, Iota, Kappa, Delta, Mu, C.1.2, as well as Omicron variants BA.1, BA.2, BA.2.75, XBB.1, BQ.1.1, EG.5.1, BA.2.86, and JN.1 in this study. Although there were no significant differences in the infection-enhancing activity, binding mode, and gene usage between the NIEAs we identified and other published NIEAs, our findings largely expanded the available pool of NIEAs in favor of summarizing the general rule of these NIEAs. It should be noted that the NIEAs identified in this study and published in previous studies have been derived from different patients in different geographic regions and age groups. Therefore, these NIEAs have been generally representative in the population.

Furthermore, these 9 NIEAs recognized similar binding regions on the NTD with those previously reported [26, 29, 30]. Due to a relatively lower binding affinity, P5S-1D12 displayed an indistinct competition with 8D2 whose binding epitopes had been well determined. However, 8D2 obviously competed with the HRP-labeled P5S-1D12. It is a common phenomenon that one antibody exhibits strong competition with another antibody, but another antibody exhibits weak or no competition with this antibody [19, 26]. Therefore, it could be considered that two antibodies recognized similar epitopes, irrespective of whether forward and/or reverse competition was observed.

Previous studies have found that some mutations in the NTD, particularly those around infection-enhancing supersite (residues 27–32, 59–66, and 211–218), are critical for antibody recognition and play a pivotal role in the infection-enhancing mechanism [26, 28, 29, 57]. These mutations account for the majority of changes in the NTD sequence of SARS-CoV-2 variants, impacting discrete domains in the NTD protein [29]. By contrast, some mutants identified in this study, such as P9L, T19A, and D80A, etc., had a relatively minor impact on the recognition of NIEAs. Moreover, Liu et al. found that the double mutants could further reduce binding of certain NIEAs than the single mutant, and the NTD with the quadruple mutant could not be recognized by any NIEAs [26]. Therefore, some NIEAs elicited by wild-type SARS-CoV-2 could still enhance the infection of variants containing these mutants.

With SARS-CoV-2 variants escaping from nAbs, prevention and treatment of infection is still a key question to be solved [58–61]. Some SARS-CoV-2 variants, such as Alpha and Delta, contained mutations particularly in the RBD, which also caused an enhanced binding ability to the ACE2 receptor [32–34]. Omicron variants had many mutations located in the NTD, which were not seen in the previous variants. These mutations contributed to the increased transmissibility and marked immune evasion of SARS-CoV-2 variants, resulted in reduced protection effectiveness of vaccines and antibodies [36–40]. In this study, our findings on NIEAs have shown that this kind of infection-enhancing immune imprint induced by the WT SARS-CoV-2 do not enhance the potential infection of subsequent Omicron variants, which alleviates some concerns for the development of antibody and vaccine. Considering the high mutation rate in the NTD and the possible NIEAs, the NTD subunit may be inappropriate for the design of novel SARS-CoV-2 vaccines.

In this study, we evaluated the infection enhancement levels of NIEAs using the pseudovirus system. However, the real virus infection may display a distinct process. This is a main limitation in the experimental model, and thus the live virus should be used in the future study to make a more comprehensive comparison. Moreover, future research on NIEAs should not be limited to those derived from wild-type infections. It remains to be explored whether SARS-CoV-2 variants also could induce this kind of NIEAs. Additionally, the accurate mechanism by which bivalent binding triggers conformational changes in the RBD is still unclear. All of these require further investigation to clarify the exact functions and mechanisms of NIEAs.

Materials and methods

Cell lines and plasmids

HEK293T cells (ATCC, CBP60439), HEK293F cells (ATCC, CBP60437), Huh7 cells (ATCC, CBP60202), and HEK293T-hACE2 cells (Yeasen, 41107ES03) were preserved in our laboratory. HEK293F cells were cultured in FreeStyle 293 expression medium (Gibco, 12338-018). The cells incubation condition was set at 37°C, 5% CO₂, and 130 rpm in incubator (Eppendorf). HEK293T, HEK293T-hACE2 and Huh7 cells were cultured in DMEM medium (Gibco, 11965-092) supplemented with 10% Fetal Bovine Serum (ExCell, FSP500), 1% Penicillin-Streptomycin (Gibco, 15140-122), and 1% HEPES (1 M) buffer (Gibco, 15630-080) under the same conditions of 37°C and 5% CO₂. Using SARS-CoV-2 wild-type (WT) spike protein full-length plasmid as the template, the NTD fragment was obtained through high-fidelity PCR. The sequences of primers were 5'-gcgcaagcttatgtt-gttcctgggtgctgctgcc-3' and 5'-ggcctctagattaaggtgatggtgatg-gtgggtggctgccgatttcagggtacacttg-3'.

Protein purification

The plasmids encoding the His-tagged protein were mixed with the transfection reagent PEI (Polysciences, 24885-2) in OPTI-MEM Reduced Serum Buffer (ThermoFisher, 31985070) and incubated for 20 min before being transfected into HEK293F cells. After incubating for 7 days at 37°C in a culture incubator, the cells were centrifuged at 4°C for 20 min at 3500 g. The supernatant was filtered through a 0.45 µm Syringe Filter (Merck millipore, SLHVR33RB) to collect the protein. The protein solution was concentrated using a 30-KD Centrifugal Filters (Merck millipore, UFC903096) concentration tube. To equilibrate, 100 µL of 20% His Monster Beads (PROTEINN, PROTN_HMBN1V00001) were added to 10 beads-volume binding buffer (50 mM Tris-HCl, pH 8.0, 500 mM NaCl, 5 mM Imidazole) and then mixed with the protein solution. The low concentration of imidazole in the binding buffer could reduce the nonspecific binding of contaminating proteins. Tris-HCl acted as the buffer, and the addition of NaCl helped maintain protein solubility and simulated physiological conditions. The mixture was stirred at room temperature for 30 min before discarding the supernatant with a magnet. Subsequently, 1 mL of washing buffer (50 mM Tris-HCl, pH 8.0, 500 mM NaCl, 20 mM Imidazole) was added and mixed at room temperature for 5 min to remove unbound proteins. Next, 10 bead-volumes of elution buffer (50 mM Tris-HCl, pH 8.0, 500 mM NaCl, 250 mM Imidazole) were added, and the mixture was pipetted up and down 10 times to elute the target protein from the His Monster Beads. The high concentration of imidazole in the elution buffer was effective in eluting the target protein. Finally, the pure target protein was collected in the supernatant

using a magnet. The eluents at each stage were subjected to detection by SDS-PAGE, and the protein concentration was determined using NanoDrop 2000 (Thermo Scientific).

Antibody preparation

Three COVID-19 convalescents infected with the wild-type SARS-CoV-2 did not have other specific clinical characteristics, and these 9 NIEAs were sourced from the antibody panel published in our previous study [46]. The selection of these 3 patients did not follow a specific standard, but there were criteria for selecting antibodies that bound to neither RBD nor S2 of the spike protein. The 9 NIEAs and control antibodies were synthesized by the company based on the antibody sequence from relevant literature and produced using the methods described in previous studies [16, 19, 21, 27, 28, 46, 62]. Monoclonal antibodies (mAbs) were produced by transiently transfecting HEK293F cells (Life Technologies) with equal quantities of paired heavy- and light-chain plasmids. The antibodies in the culture supernatant were purified through affinity chromatography using Protein A column (Senhui, 14-0010-04). The column was equilibrated with 10 columns-volume of PBS. Then the filtered supernatant was added to the column, and after complete binding, unbound proteins were washed away with 10 columns-volume of PBS. The target antibodies were then eluted with 10 mL of Elution Buffer pH 3.0 (Sangon Biotech, C600481-0500) and mixed with 1 mL of 1 M Tris-HCl Solution pH 8.5 (Sangon Biotech, B548141-0500) to adjust the pH. Following concentration using a 30-KD ultrafiltration tube, PBS was added to exchange the solution three times and impurities were filtered out using a 0.22 μm Centrifuge Tube Filter (Costar, 98231-UT-1) to better preserve the antibodies, which were then stored at -80°C . The concentrations and purity were determined using a NanoDrop2000 (Thermo Scientific).

To generate Fab fragments, IgG was digested with immobilized papain (Sigma-Aldrich, P4762-1G) at 37°C for 12 hours in the presence of 20 mM L-Cysteine hydrochloride (Sigma-Aldrich, 30120-50G) and 20 mM EDTA (Invitrogen, 15575-038). Then the reaction was terminated by adding 0.5 M Iodoacetamide (Sigma-Aldrich, I6125-25G) [63]. After that, the mixture was passed through Protein A column to remove Fc fragments and undigested IgG. The F(ab')_2 fragments were prepared and purified according to the manufacturer's protocol of F(ab')_2 Preparation Kit (Thermo Scientific, 44988).

Enzyme linked immunosorbent assay (ELISA)

Wild-type SARS-CoV-2 spike protein trimer and NTD protein solutions were diluted to a concentration of 2 $\mu\text{g}/\text{mL}$ in PBS and coated at 100 μL per well of a 96-well plate, incubated overnight at 4°C . The samples were

washed three times with PBS-T (PBS containing 0.05% Tween-20). Blocking was performed at room temperature with blocking buffer containing 5% NON-Fat Powdered Milk (Sangon Biotech, A600669-0250) and 2% bovine serum albumin (Sangon Biotech, A600332-0100) in PBS, 200 μL per well for 1 h. Samples were washed three times with PBST. The antibodies to be tested were diluted starting from 10 $\mu\text{g}/\text{mL}$ and serially diluted five times for a total of eight gradients, adding 100 μL to each well of the ELISA plate and incubating at 37°C for 1 h. Samples were washed five times with PBS-T. Then, 100 μL of HRP-conjugated goat anti-human IgG antibody (ZS, ZB-2304), diluted 1:5000 in blocking buffer, was added to each well and incubated at 37°C for 1 h. Samples were again washed five times with PBS-T. The ELISA Color Colution (Sangon Biotech, E661007-0100) was added to each well and incubated at room temperature in the dark for 20 min. The reaction was terminated by adding 50 μL of 2M H_2SO_4 per well. The optical density (OD) values were measured at 450 nm using a Varioskan LUX multimode microplate reader (Thermo Scientific). Previously published antibodies targeting the SARS-CoV-2 WT NTD were used as controls.

Competition enzyme linked immunosorbent assay

The 8D2 [19] and P5S-1D12 antibodies were labeled using an HRP conjugation kit (Abcam, ab201795) and stored at -20°C before detected [64, 65]. The 96-well plates were coated with wild-type SARS-CoV-2 spike trimer protein, and incubated at 4°C overnight. The plates were washed three times with PBST buffer and blocked with PBS containing 5% NON-Fat Powdered Milk and 2% BSA in PBS for 1 h at room temperature. The antibodies to be detected were serially diluted, mixed with an equal volume of the HRP labeled 8D2 or P5S-1D12 antibodies, and added to the 96-well plate for incubation at 37°C for 1 h. Finally, the ELISA Color Colution was added to the plates and incubated for 20 min at room temperature in the dark before terminating the reaction with 2M H_2SO_4 . The readout was detected at a wavelength of 450 nm using a Varioskan LUX multifunctional microplate reader (Thermo Scientific). The previously published HIV-1 targeting antibody VRC01 [62] was used as a negative control.

Packaging and infectivity testing of SARS-CoV-2 pseudoviruses

HEK293T cells were incubated overnight in DMEM culture medium (10% Fetal Bovine Serum, 1% HEPES) without antibiotics in a 5% CO_2 incubator at 37°C . Once the cell density reached around 80%, transfection was performed. The plasmid and EZ transfection reagent were mixed at a 1:3 ratio in OPTI-MEM Reduced Serum Buffer and incubated for 10 min at room temperature. The

mixed solution was added dropwise to HEK293T cells cultured in antibiotic-free medium. After incubating for 6 h at 37°C, the medium containing the EZ Trans-DNA complexes was removed and replaced with fresh culture medium, and cells were incubated for an additional 48 h before the supernatant was collected. Cell supernatants were centrifuged at 4 °C, 1000 g for 10 min, filtered, and stored at -80°C [45, 66, 67].

To measure the titer of the packaged pseudoviruses, 40 µL of pseudovirus solution was added to 110 µL of DMEM complete culture medium (containing 10% Fetal Bovine Serum, 1% HEPES, and 1% Penicillin Streptomycin) to achieve a 2-fold dilution. This mixture was then incubated at 37°C for 1 h. The medium without pseudovirus was served as the virus control. Subsequently, the mixture was added to the cell solution of HEK293T-hACE2 containing 2.5×10^4 cells/well and DEAE-dextran at a 1:1000 ratio in 96 white cell culture wells and incubated for 48 h at 37°C. The culture medium was then removed, and 100 µL of the Bright-Lite Luciferase reagent (Vazyme Biotech, DD1204-03-AA) was added. The plate was shaken for 2 min at room temperature before the luciferase activity was measured using the Varioskan LUX multimode microplate reader (Thermo Fisher). All pseudoviruses have been validated by sequencing, and detailed sequence information of spike proteins used were listed below.

SARS-CoV-2 wild-type (WT).

Accession number: NC_045512.

SARS-CoV-2 Alpha.

Accession number: EPI_ISL_600093.

SARS-CoV-2 Beta.

Accession number: EPI_ISL_660637.

SARS-CoV-2 Lota.

Accession number: EPI_ISL_1708781.

SARS-CoV-2 Kappa.

Accession number: EPI_ISL_2741391.

SARS-CoV-2 Delta.

Accession number: EPI_ISL_1409773.

SARS-CoV-2 Mu.

Accession number: EPI_ISL_4659819.

SARS-CoV-2 C.1.2.

P9L, C136F, 144–145 del, R190S, D215G.

SARS-CoV-2 Omicron BA.1.

Accession number: EPI_ISL_6699736.

SARS-CoV-2 Omicron BA.2.

Accession number: EPI_ISL_9652748.

SARS-CoV-2 Omicron BA.2.75.

Accession number: EPI_ISL_13502576.

SARS-CoV-2 Omicron XBB.1.

Accession number: EPI_ISL_14917761.

SARS-CoV-2 Omicron BQ.1.1.

Accession number: EPI_ISL_14818139.

SARS-CoV-2 Omicron EG.5.1.

Accession number: EPI_ISL_17854292.

SARS-CoV-2 Omicron BA.2.86.

Accession number: EPI_ISL_18110065.

SARS-CoV-2 Omicron JN.1.

Accession number: EPI_ISL_18313756.

Pseudovirus infection experiment

To measure the infection-enhancing ability of antibodies, the concentration of the test antibodies was prepared starting from 50 µg/mL and serially diluted five times, for a total of eight gradients, with the last column containing control medium without antibodies [45, 68]. Equal volumes of the diluted antibody solution were mixed with SARS-CoV-2 pseudovirus solution and incubated at 37 °C for 1 h. A cell solution of HEK293T-hACE2 containing 3×10^4 cells/well and DEAE-dextran at 1:1000 was prepared using DMEM complete medium. The pseudovirus mixture was added at 100 µL per well to a white 96-well plate, followed by 100 µL of the prepared cell solution. After 48 h of incubation at 37 °C, the medium was removed and 100 µL of Bright-Lite luciferase reagent (Vazyme Biotech) was added to each well. The fluorescence signal was measured after a 2-minute incubation at room temperature using a Varioskan LUX multimode microplate reader (Thermo Scientific). The 50% effect concentration (EC_{50}) was calculated using GraphPad Prism 8.0 software with the model of log vs. normalized response-variable slope.

Flow cytometric analysis of antibodies

The plasmid expressing the Flag-WT NTD-PDGFRβ TM was transfected into HEK293T cells. The cells were stained with the Zombie Violet Fixable Viability Kit (Biolegend, 423114) to exclude dead cells, and incubated with the mAbs and PE anti-DYKDDDDK Tag antibody (Biolegend, 637309), followed by APC-conjugated anti-human IgG antibody (Invitrogen, A21445). Then, the antibodies bound to the stained cells were analyzed by flow cytometers. Antibody binding to the Flag-positive cells were shown in the figures analyzed by the FlowJo software.

Gene family usage analysis of monoclonal antibodies

The program IMGT/V-QUEST (<http://www.imgt.org/IMG/vquest>) was used to analyze the germline genes, the degree of somatic hypermutation (SHM), and the loop of complementarity determining region 3 (CDR3) of each mAbs [65, 69].

Binding affinity of antibodies measured by surface plasmon resonance (SPR)

The binding affinity of mAbs to the SARS-CoV-2 NTD were analyzed using SPR (GE Healthcare)[63]. Specifically, the purified NTD was covalently immobilized onto a CM5 sensor chip (Cytiva, 29149603) through amino

groups in 10 mM sodium acetate buffer pH 5.0 (Cytiva, BR100351), achieving a final response unit (RU) of approximately 250. The sensorgrams were fitted to a 1:1 binding model using the BIA evaluation software (GE Healthcare).

Statistical analysis

The statistical significance was performed using two-tailed paired Wilcoxon test. $**p < 0.01$; $*p < 0.05$.

Supplementary Information

The online version contains supplementary material available at <https://doi.org/10.1186/s12985-025-02667-0>.

Supplementary Material 1

Acknowledgements

The authors wish to thank the biological sample bank of the Shenzhen Third People's Hospital for bio-samples and services provided.

Author contributions

Z.Z. and B.J. conceived and designed the study. Q.G., H.W., and C.L. performed most of experiments and analyzed the data together with assistance from W.L., B.Z., S.T., Q.F., and X.G.. Q.G., H.W., C.L., B.J., and Z.Z. participated in discussion of the results and wrote the manuscript. All authors read and approved this version of manuscript.

Funding

This study was supported by the National Natural Science Foundation of China (82025022 and 92169204 to Z.Z., 82322040 and 82171752 to B.J.); the Guangdong Basic and Applied Basic Research Foundation (2021B1515020034 to B.J.); the Shenzhen Science and Technology Program (RCYX20200714114700046 to B.J., ZDSYS20210623091810030 to Z.Z.); the Science and Technology Innovation Committee of Shenzhen Municipality (JCYJ20220530163014031 to H.W., JCYJ20200109144201725 to Z.Z., JCYJ20210324132003010 to C.L.); the Chinese Academy of Medical Sciences Clinical and Translational Medicine Research Project (2022-I2M-C&T-B-113 to Z.Z.); and the Shenzhen High-level Hospital Construction Fund (23250G1002 to B.J.).

Data availability

No datasets were generated or analysed during the current study.

Declarations

Ethics approval and consent to participate

This study was approved by the Ethics Committee of Shenzhen Third People's Hospital, China (approval number: 2021-030). The biological sample bank of the Shenzhen Third People's Hospital supplied the participant's samples and clinical information.

Consent for publication

All authors approved the submission of the manuscript for publication.

Competing interests

The authors declare no competing interests.

Author details

¹Department of Infectious Diseases, Affiliated Hospital of Southwest Medical University, Luzhou 646000, China

²Institute for Hepatology, National Clinical Research Center for Infectious Disease, Shenzhen Third People's Hospital, The Second Affiliated Hospital, School of Medicine, Southern University of Science and Technology, Shenzhen, Guangdong Province 518112, China

³Guangdong Key Laboratory for Anti-infection Drug Quality Evaluation, Shenzhen, Guangdong Province 518112, China

⁴Shenzhen Research Center for Communicable Disease Diagnosis and Treatment, Chinese Academy of Medical Sciences, Shenzhen, Guangdong Province 518112, China

Received: 23 November 2024 / Accepted: 12 February 2025

Published online: 24 February 2025

References

1. Stadler K, Masignani V, Eickmann M, Becker S, Abrignani S, Klenk HD, Rap-puoli R. SARS—beginning to understand a new virus. *Nat Rev Microbiol*. 2003;1(3):209–18.
2. Mackay IM, Arden KE. MERS coronavirus: diagnostics, epidemiology and transmission. *Virology*. 2015;12:222.
3. Wu F, Zhao S, Yu B, Chen YM, Wang W, Song ZG, Hu Y, Tao ZW, Tian JH, Pei YY, Yuan ML, Zhang YL, Dai FH, Liu Y, Wang QM, Zheng JJ, Xu L, Holmes EC, Zhang YZ. A new coronavirus associated with human respiratory disease in China. *Nature*. 2020;579(7798):265–9.
4. Banerjee A, Kulcsar K, Misra V, Frieman M, Mossman K. Bats and coronaviruses. *Viruses* 2019, 11 (1).
5. Wong ACP, Li X, Lau SKP, Woo PCY. Global epidemiology of Bat coronaviruses. *Viruses* 2019, 11 (2).
6. Zhu N, Zhang D, Wang W, Li X, Yang B, Song J, Zhao X, Huang B, Shi W, Lu R, Niu P, Zhan F, Ma X, Wang D, Xu W, Wu G, Gao GF, Tan W. A novel coronavirus from patients with Pneumonia in China, 2019. *N Engl J Med*. 2020;382(8):727–33.
7. Goh GK, Dunker AK, Foster JA, Uversky VN. Rigidity of the Outer Shell Predicted by a Protein Intrinsic Disorder Model Sheds Light on the COVID-19 (Wuhan-2019-nCoV) Infectivity. *Biomolecules* 2020, 10 (2).
8. Puelles VG, Lütgehetmann M, Lindenmeyer MT, Sperhake JP, Wong MN, Allweiss L, Chilla S, Heinemann A, Wanner N, Liu S, Braun F, Lu S, Pfefferle S, Schröder AS, Edler C, Gross O, Glatzel M, Wichmann D, Wüthrich T, Kluge S, Püschel K, Aepfelbacher M, Huber TB. Multiorgan and renal tropism of SARS-CoV-2. *N Engl J Med*. 2020;383(6):590–2.
9. Lamers MM, Beumer J, van der Vaart J, Knops K, Puschhof J, Breugem TI, Ravelli RBG, van Paul J, Mykytyn AZ, Duimel HQ, van Donselaar E, Riesebosch S, Kuijpers HJH, Schipper D, van de Wetering WJ, de Graaf M, Koopmans M, Cuppen E, Peters PJ, Haagmans BL, Clevers H. SARS-CoV-2 productively infects human gut enterocytes. *Science*. 2020;369(6499):50–4.
10. Walls AC, Park YJ, Tortorici MA, Wall A, McGuire AT, Veesler D. Structure, function, and Antigenicity of the SARS-CoV-2 Spike Glycoprotein. *Cell*. 2020;181(2):281–e2926.
11. Abdelrahman Z, Li M, Wang X. Comparative review of SARS-CoV-2, SARS-CoV, MERS-CoV, and Influenza a respiratory viruses. *Front Immunol*. 2020;11:552909.
12. Zhang J, Xiao T, Cai Y, Chen B. Structure of SARS-CoV-2 spike protein. *Curr Opin Virol*. 2021;50:173–82.
13. Yan R, Zhang Y, Li Y, Xia L, Guo Y, Zhou Q. Structural basis for the recognition of SARS-CoV-2 by full-length human ACE2. *Science*. 2020;367(6485):1444–8.
14. Hoffmann M, Kleine-Weber H, Schroeder S, Krüger N, Herrler T, Erichsen S, Schiergens TS, Herrler G, Wu NH, Nitsche A, Müller MA, Drosten C, Pöhlmann S. SARS-CoV-2 cell entry depends on ACE2 and TMPRSS2 and is blocked by a clinically proven protease inhibitor. *Cell*. 2020;181(2):271–e2808.
15. Benton DJ, Wrobel AG, Xu P, Roustan C, Martin SR, Rosenthal PB, Skehel JJ, Gamblin SJ. Receptor binding and priming of the spike protein of SARS-CoV-2 for membrane fusion. *Nature*. 2020;588(7837):327–30.
16. Cao Y, Yisimayi A, Jian F, Song W, Xiao T, Wang L, Du S, Wang J, Li Q, Chen X, Yu Y, Wang P, Zhang Z, Liu P, An R, Hao X, Wang Y, Wang J, Feng R, Sun H, Zhao L, Zhang W, Zhao D, Zheng J, Yu L, Li C, Zhang N, Wang R, Niu X, Yang S, Song X, Chai Y, Hu Y, Shi Y, Zheng L, Li Z, Gu Q, Shao F, Huang W, Jin R, Shen Z, Wang Y, Wang X, Xiao J, Xie XS. BA.2.12.1, BA.4 and BA.5 escape antibodies elicited by Omicron infection. *Nature*. 2022;608(7923):593–602.
17. Noy-Porat T, Mechaly A, Levy Y, Makdasi E, Alcalay R, Gur D, Aftalion M, Falach R, Leviatan Ben-Arye S, Lazar S, Zauberman A, Epstein E, Chitlaru T, Weiss S, Achdout H, Edgeworth JD, Kikkeri R, Yu H, Chen X, Yitzhaki S, Shapira SC, Padler-Karavani V, Mazor O, Rosenfeld R. Therapeutic antibodies, targeting the SARS-CoV-2 spike N-terminal domain, protect lethally infected K18-hACE2 mice. *iScience* 2021, 24 (5), 102479.
18. Wang Z, Muecksch F, Cho A, Gaebler C, Hoffmann HH, Ramos V, Zong S, Cipolla M, Johnson B, Schmidt F, DaSilva J, Bednarski E, Ben Tanfous T, Raspe R, Yao K, Lee YE, Chen T, Turroja M, Milard KG, Dizon J, Kaczynska A, Gazumyan

- A, Oliveira TY, Rice CM, Caskey M, Bieniasz PD, Hatzioannou T, Barnes CO, Nussenzweig MC. Analysis of memory B cells identifies conserved neutralizing epitopes on the N-terminal domain of variant SARS-CoV-2 spike proteins. *Immunity*. 2022;55(6):998–e10128.
19. Chi X, Yan R, Zhang J, Zhang G, Zhang Y, Hao M, Zhang Z, Fan P, Dong Y, Yang Y, Chen Z, Guo Y, Zhang J, Li Y, Song X, Chen Y, Xia L, Fu L, Hou L, Xu J, Yu C, Li J, Zhou Q, Chen W. A neutralizing human antibody binds to the N-terminal domain of the spike protein of SARS-CoV-2. *Science*. 2020;369(6504):650–5.
20. Li Y, Wang T, Zhang J, Shao B, Gong H, Wang Y, He X, Liu S, Liu TY. Exploring the Regulatory function of the N-terminal domain of SARS-CoV-2 spike protein through Molecular Dynamics Simulation. *Adv Theory Simul*. 2021;4(10):2100152.
21. Sun X, Yi C, Zhu Y, Ding L, Xia S, Chen X, Liu M, Gu C, Lu X, Fu Y, Chen S, Zhang T, Zhang Y, Yang Z, Ma L, Gu W, Hu G, Du S, Yan R, Fu W, Yuan S, Qiu C, Zhao C, Zhang X, He Y, Qu A, Zhou X, Li X, Wong G, Deng Q, Zhou Q, Lu H, Ling Z, Ding J, Lu L, Xu J, Xie Y, Sun B. Neutralization mechanism of a human antibody with pan-coronavirus reactivity including SARS-CoV-2. *Nat Microbiol*. 2022;7(7):1063–74.
22. Dacon C, Tucker C, Peng L, Lee CD, Lin TH, Yuan M, Cong Y, Wang L, Purser L, Williams JK, Pyo CW, Kosik I, Hu Z, Zhao M, Mohan D, Cooper AJR, Peterson M, Skinner J, Dixit S, Kollins E, Huzella L, Perry D, Byrum R, Lembirik S, Drawbaugh D, Eaton B, Zhang Y, Yang ES, Chen M, Leung K, Weinberg RS, Pegu A, Geraghty DE, Davidson E, Douagi I, Moir S, Yewdell JW, Schmaljohn C, Crompton PD, Holbrook MR, Nemazee D, Masciola JR, Wilson IA, Tan J. Broadly neutralizing antibodies target the coronavirus fusion peptide. *Science*. 2022;377(6607):728–35.
23. Low JS, Jerak J, Tortorici MA, McCallum M, Pinto D, Cassotta A, Foglierini M, Mele F, Abdelnabi R, Weynand B, Noack J, Montiel-Ruiz M, Bianchi S, Benigni F, Sprugasci N, Joshi A, Bowen JE, Stewart C, Rexhepaj M, Walls AC, Jarrossay D, Morone D, Paparoditis P, Garzoni C, Ferrari P, Ceschi A, Neyts J, Purcell LA, Snell G, Corti D, Lanzavecchia A, Veester D, Sallusto F. ACE2-binding exposes the SARS-CoV-2 fusion peptide to broadly neutralizing coronavirus antibodies. *Science*. 2022;377(6607):735–42.
24. Chen Y, Zhao X, Zhou H, Zhu H, Jiang S, Wang P. Broadly neutralizing antibodies to SARS-CoV-2 and other human coronaviruses. *Nat Rev Immunol*. 2023;23(3):189–99.
25. Qi H, Liu B, Wang X, Zhang L. The humoral response and antibodies against SARS-CoV-2 infection. *Nat Immunol*. 2022;23(7):1008–20.
26. Liu Y, Soh WT, Kishikawa JI, Hirose M, Nakayama EE, Li S, Sasai M, Suzuki T, Tada A, Arakawa A, Matsuoka S, Akamatsu K, Matsuda M, Ono C, Torii S, Kishida K, Jin H, Nakai W, Arase N, Nakagawa A, Matsumoto M, Nakazaki Y, Shindo Y, Kohyama M, Tomii K, Ohmura K, Ohshima S, Okamoto T, Yamamoto M, Nakagami H, Matsuura Y, Nakagawa A, Kato T, Okada M, Standley DM, Shioda T, Arase H. An infectivity-enhancing site on the SARS-CoV-2 spike protein targeted by antibodies. *Cell*. 2021;184(13):3452–e346618.
27. Zost SJ, Gilchuk P, Chen RE, Case JB, Reidy JX, Trivette A, Nargi RS, Sutton RE, Suryadevara N, Chen EC, Binshtein S, Shrihari S, Ostrowski M, Chu HY, Didier JE, MacRenaris KW, Jones T, Day S, Myers L, Eun-Hyung Lee F, Nguyen DC, Sanz I, Martinez DR, Rothlauf PW, Bloyet LM, Whelan SPJ, Baric RS, Thackray LB, Diamond MS, Carnahan RH, Crowe JE Jr. Rapid isolation and profiling of a diverse panel of human monoclonal antibodies targeting the SARS-CoV-2 spike protein. *Nat Med*. 2020;26(9):1422–7.
28. Li D, Edwards RJ, Manne K, Martinez DR, Schäfer A, Alam SM, Wiehe K, Lu X, Parks R, Sutherland LL, Oguin TH 3rd, McDanal C, Perez LG, Mansouri K, Gobeil SMC, Janowska K, Stalls V, Kopp M, Cai F, Lee E, Foulger A, Hernandez GE, Sanzone A, Tilahun K, Jiang C, Tse LV, Bock KW, Minai M, Nagata BM, Cronin K, Gee-Lai V, Deyton M, Barr M, Von Holle T, Macintyre AN, Stover E, Feldman J, Hauser BM, Caradonna TM, Scobey TD, Rountree W, Wang Y, Moody MA, Cain DW, DeMarco CT, Denny TN, Woods CW, Petzold EW, Schmidt AG, Teng IT, Zhou T, Kwong PD, Masciola JR, Graham BS, Moore IN, Seder R, Andersen H, Lewis MG, Montefiori DC, Sempowski GD, Baric RS, Acharya P, Haynes BF, Saunders. In vitro and in vivo functions of SARS-CoV-2 infection-enhancing and neutralizing antibodies. *Cell*. 2021;184(16):4203–e421932. K. O.
29. Connor RI, Sakharkar M, Rappazzo CG, Kaku CI, Curtis NC, Shin S, Wieland-Alter WF, Wentworth J, Mielcarz DW, Weiner JA, Ackerman ME, Walker LM, Lee J, Wright PF. Characteristics and functions of infection-enhancing antibodies to the N-terminal domain of SARS-CoV-2. *Pathog Immun*. 2024;9(2):1–24.
30. Lusiany T, Terada T, Kishikawa JI, Hirose M, Chen DV, Sugihara F, Ismanto HS, van Eerden FJ, Li S, Kato T, Arase H, Yoshiharu M, Okada M, Standley DM. Enhancement of SARS-CoV-2 infection via Crosslinking of adjacent spike proteins by N-Terminal domain-targeting antibodies. *Viruses*. 2023;15:12.
31. Qu P, Xu K, Faraone JN, Goodarzi N, Zheng YM, Carlin C, Bednash JS, Horowitz JC, Mallampalli RK, Saif LJ, Oltz EM, Jones D, Gumina RJ, Liu SL. Immune evasion, infectivity, and fusogenicity of SARS-CoV-2 BA.2.86 and FLiP variants. *Cell*. 2024;187(3):585–e5956.
32. McCallum M, Walls AC, Sprouse KR, Bowen JE, Rosen LE, Dang HV, De Marco A, Franko N, Tilles SW, Logue J, Miranda MC, Ahlrichs M, Carter L, Snell G, Pizzuto MS, Chu HY, Van Voorhis WC, Corti D, Veester D. Molecular basis of immune evasion by the Delta and Kappa SARS-CoV-2 variants. *Science*. 2021;374(6575):1621–6.
33. Kraemer MUG, Hill V, Ruis C, Dellicour S, Bajaj S, McCrone JT, Baele G, Parag KV, Battle AL, Gutierrez B, Jackson B, Colquhoun R, O'Toole Á, Klein B, Vespignani A, Volz E, Faria NR, Aanensen DM, Loman NJ, du Plessis L, Cauchemez S, Rambaut A, Scarpino SV, Pybus OG. Spatiotemporal invasion dynamics of SARS-CoV-2 lineage B.1.1.7 emergence. *Science*. 2021;373(6557):889–95.
34. Ferreira I, Kemp SA, Datir R, Saito A, Meng B, Rakshit B, Takaoiri-Kondo A, Kosugi Y, Uriu K, Kimura I, Shirakawa K, Abdullahi A, Agarwal A, Ozono S, Tokunaga K, Sato K, Gupta RK. SARS-CoV-2 B.1.617 mutations L452R and E484Q are not synergistic for antibody evasion. *J Infect Dis*. 2021;224(6):989–94.
35. Huang M, Wu L, Zheng A, Xie Y, He Q, Rong X, Han P, Du P, Han P, Zhang Z, Zhao R, Jia Y, Li L, Bai B, Hu Z, Hu S, Niu S, Hu Y, Liu H, Liu B, Cui K, Li W, Zhao X, Liu K, Qi J, Wang Q, Gao GF. Atlas of currently available human neutralizing antibodies against SARS-CoV-2 and escape by Omicron sub-variants BA.1/BA.1.1/BA.2/BA.3. *Immunity* 2022, 55 (8), 1501–1514.e3.
36. Yamasoba D, Kimura I, Nasser H, Morioka Y, Nao N, Ito J, Uriu K, Tsuda M, Zahradnik J, Shirakawa K, Suzuki R, Kishimoto M, Kosugi Y, Kobiyama K, Hara T, Toyoda M, Tanaka YL, Butleranaka EP, Shimizu R, Ito H, Wang L, Oda Y, Orba Y, Sasaki M, Nagata K, Yoshimatsu K, Asakura H, Nagashima M, Sadamasu K, Yoshimura K, Kuramochi J, Seki M, Fujiki R, Kaneda A, Shimada T, Nakada TA, Sakao S, Suzuki T, Ueno T, Takaori-Kondo A, Ishii KJ, Schreiber G, Sawa H, Saito A, Irie T, Tanaka S, Matsuno K, Fukuhara T, Ikeda T, Sato K. Virological characteristics of the SARS-CoV-2 Omicron BA.2 spike. *Cell*. 2022;185(12):2103–e211519.
37. Cameron E, Bowen JE, Rosen LE, Saliba C, Zepeda SK, Culap K, Pinto D, VanBlargan LA, De Marco A, di Iulio J, Zatta F, Kaiser H, Noack J, Farhat N, Czudnochowski N, Havenar-Daughton C, Sprouse KR, Dillen JR, Powell AE, Chen A, Maher C, Yin L, Sun D, Soriaga L, Bassi J, Silacci-Fregni C, Gustafsson C, Franko NM, Logue J, Iqbal NT, Mazzitelli I, Geffner J, Grifantini R, Chu H, Gori A, Riva A, Giannini O, Ceschi A, Ferrari P, Cippà PE, Franzetti-Pellanda A, Garzoni C, Halfmann PJ, Kawaoka Y, Hebner C, Purcell LA, Piccoli L, Pizzuto MS, Walls AC, Diamond MS, Telenti A, Virgin HW, Lanzavecchia A, Snell G, Veester D, Corti D. Broadly neutralizing antibodies overcome SARS-CoV-2 Omicron antigenic shift. *Nature* 2022, 602 (7898), 664–670.
38. Cao Y, Wang J, Jian F, Xiao T, Song W, Yisimayi A, Huang W, Li Q, Wang P, An R, Wang J, Wang Y, Niu X, Yang S, Liang H, Sun H, Li T, Yu Y, Cui Q, Liu S, Yang X, Du S, Zhang Z, Hao X, Shao F, Jin R, Wang X, Xiao J, Wang Y, Xie XS. Omicron escapes the majority of existing SARS-CoV-2 neutralizing antibodies. *Nature*. 2022;602(7898):657–63.
39. Kaku Y, Okumura K, Padilla-Blanco M, Kosugi Y, Uriu K, Hinay AA Jr., Chen L, Plianchaisuk A, Kobiyama K, Ishii KJ, Zahradnik J, Ito J, Sato K. Virological characteristics of the SARS-CoV-2 JN.1 variant. *Lancet Infect Dis* 2024, 24 (2), e82.
40. Wannigama DL, Amarasiri M, Phattharapornjaroen P, Hurst C, Modchang C, Chadsuthi S, Anupong S, Miyanaga K, Cui L, Fernandez S, Huang AT, Ounjai P, Singer AC, Ragupathi NKD, Sano D, Furukawa T, Sei K, Leelahavanichkul A, Kanjanabuch T, Chatsuwat T, Higgings PG, Nanbo A, Kicic A, Siow R, Trowsdale S, Hongsing P, Khatib A, Shibuya K, Abe S, Ishikawa H. Increased faecal shedding in SARS-CoV-2 variants BA.2.86 and JN.1. *Lancet Infect Dis*. 2024;24(6):e348–50.
41. Planas D, Staropoli I, Michel V, Lemoine F, Donati F, Prot M, Porrot F, Guivel-Benhassine F, Jeyarajah B, Brisebarre A, Dehan O, Avon L, Bolland WH, Hubert M, Buchrieser J, Vanhoucke T, Rosenbaum P, Veyer D, Péré H, Lina B, Trouillet-Assant S, Hocqueloux L, Prazuck T, Simon-Loriere E, Schwartz O. Distinct evolution of SARS-CoV-2 Omicron XBB and BA.2.86/JN.1 lineages combining increased fitness and antibody evasion. *Nat Commun*. 2024;15(1):2254.
42. Yang S, Yu Y, Xu Y, Jian F, Song W, Yisimayi A, Wang P, Wang J, Liu J, Yu L, Niu X, Wang J, Wang Y, Shao F, Jin R, Wang Y, Cao Y. Fast evolution of SARS-CoV-2 BA.2.86 to JN.1 under heavy immune pressure. *Lancet Infect Dis*. 2024;24(2):e70–2.
43. Han X, Ye Q. The variants of SARS-CoV-2 and the challenges of vaccines. *J Med Virol*. 2022;94(4):1366–72.
44. He P, Liu B, Gao X, Yan Q, Pei R, Sun J, Chen Q, Hou R, Li Z, Zhang Y, Zhao J, Sun H, Feng B, Wang Q, Yi H, Hu P, Li P, Zhang Y, Chen Z, Niu X, Zhong X, Jin

- L, Liu X, Qu K, Ciazynska KA, Carter AP, Briggs JAG, Chen J, Liu J, Chen X, He J, Chen L, Xiong X. SARS-CoV-2 Delta and Omicron variants evade population antibody response by mutations in a single spike epitope. *Nat Microbiol*. 2022;7(10):1635–49.
45. Ju B, Zheng Q, Guo H, Fan Q, Li T, Song S, Sun H, Shen S, Zhou X, Xue W, Cui L, Zhou B, Li S, Xia N, Zhang Z. Immune escape by SARS-CoV-2 Omicron variant and structural basis of its effective neutralization by a broad neutralizing human antibody VacW-209. *Cell Res*. 2022;32(5):491–4.
46. Ju B, Zhang Q, Wang Z, Aw ZQ, Chen P, Zhou B, Wang R, Ge X, Lv Q, Cheng L, Zhang R, Wong YH, Chen H, Wang H, Shan S, Liao X, Shi X, Liu L, Chu JJH, Wang X, Zhang Z, Zhang L. Infection with wild-type SARS-CoV-2 elicits broadly neutralizing and protective antibodies against omicron subvariants. *Nat Immunol*. 2023;24(4):690–9.
47. Cai Y, Zhang J, Xiao T, Lavine CL, Rawson S, Peng H, Zhu H, Anand K, Tong P, Gautam A, Lu S, Sterling SM, Walsh RM, Jr., Rits-Volloch S, Lu J, Wesemann DR, Yang W, Seaman MS, Chen B. Structural basis for enhanced infectivity and immune evasion of SARS-CoV-2 variants. *Science* 2021, 373 (6555), 642–648.
48. Deng X, Garcia-Knight MA, Khalid MM, Servellita V, Wang C, Morris MK, Sotomayor-González A, Glasner DR, Reyes KR, Gliwa AS, Reddy NP, Sanchez San Martin C, Federman S, Cheng J, Balcerek J, Taylor J, Streithorst JA, Miller S, Sreekumar B, Chen PY, Schulze-Gahmen U, Taha TY, Hayashi JM, Simoneau CR, Kumar GR, McMahon S, Lidsky PV, Xiao Y, Hemarajata P, Green NM, Espinosa A, Kath C, Haw M, Bell J, Hacker JK, Hanson C, Wadford DA, Anaya C, Ferguson D, Frankino PA, Shivram H, Lareau LF, Wyman SK, Ott M, Andino R, Chiu CY. Transmission, infectivity, and neutralization of a spike L452R SARS-CoV-2 variant. *Cell*. 2021;184(13):3426–e34378.
49. Klinakis A, Couronia Z, Rampias T. N-terminal domain mutations of the spike protein are structurally implicated in epitope recognition in emerging SARS-CoV-2 strains. *Comput Struct Biotechnol J*. 2021;19:5556–67.
50. Vennema H, de Groot RJ, Harbourn DA, Dalderup M, Gruffydd-Jones T, Horzinek MC, Spaan WJ. Early death after feline infectious peritonitis virus challenge due to recombinant vaccinia virus immunization. *J Virol*. 1990;64(3):1407–9.
51. Shimizu J, Sasaki T, Koketsu R, Morita R, Yoshimura Y, Murakami A, Saito Y, Kusunoki T, Samune Y, Nakayama EE, Miyazaki K, Shioda T. Reevaluation of antibody-dependent enhancement of infection in anti-SARS-CoV-2 therapeutic antibodies and mRNA-vaccine antisera using FcR- and ACE2-positive cells. *Sci Rep*. 2022;12(1):15612.
52. Shukla R, Ramasamy V, Shanmugam RK, Ahuja R, Khanna N. Antibody-dependent enhancement: a challenge for developing a safe Dengue Vaccine. *Front Cell Infect Microbiol*. 2020;10:572681.
53. Kapikian AZ, Mitchell RH, Chanock RM, Shvedoff RA, Stewart CE. An epidemiologic study of altered clinical reactivity to respiratory syncytial (RS) virus infection in children previously vaccinated with an inactivated RS virus vaccine. *Am J Epidemiol*. 1969;89(4):405–21.
54. Jaume M, Yip MS, Cheung CY, Leung HL, Li PH, Kien F, Dutry I, Callendret B, Escriou N, Altmeyer R, Nal B, Daëron M, Bruzzone R, Peiris JS. Anti-severe acute respiratory syndrome coronavirus spike antibodies trigger infection of human immune cells via a pH- and cysteine protease-independent FcγR pathway. *J Virol*. 2011;85(20):10582–97.
55. Wang SF, Tseng SP, Yen CH, Yang JY, Tsao CH, Shen CW, Chen KH, Liu FT, Liu WT, Chen YM, Huang JC. Antibody-dependent SARS coronavirus infection is mediated by antibodies against spike proteins. *Biochem Biophys Res Commun*. 2014;451(2):208–14.
56. Pierre CN, Adams LE, Higgins JS, Anasti K, Goodman D, Mielke D, Stanfield-Oakley S, Powers JM, Li D, Rountree W, Wang Y, Edwards RJ, Alam SM, Ferrari G, Tomaras GD, Haynes BF, Baric RS, Saunders KO. Non-neutralizing SARS-CoV-2 N-terminal domain antibodies protect mice against severe disease using Fc-mediated effector functions. *PLoS Pathog* 2024, 20 (6), e1011569.
57. Gerdol M, Dishnica K, Giorgetti A. Emergence of a recurrent insertion in the N-terminal domain of the SARS-CoV-2 spike glycoprotein. *Virus Res*. 2022;310:198674.
58. Yuan S, Ye ZW, Liang R, Tang K, Zhang AJ, Lu G, Ong CP, Man Poon VK, Chan CC, Mok BW, Qin Z, Xie Y, Chu AW, Chan WM, Ip JD, Sun H, Tsang JO, Yuen TT, Chik KK, Chan CC, Cai JP, Luo C, Lu L, Yip CC, Chu H, To KK, Chen H, Jin DY, Yuen KY, Chan JF. Pathogenicity, transmissibility, and fitness of SARS-CoV-2 Omicron in Syrian hamsters. *Science*. 2022;377(6604):428–33.
59. Xia H, Zou J, Kurhade C, Cai H, Yang Q, Cutler M, Cooper D, Muik A, Jansen KU, Xie X, Swanson KA, Shi PY. Neutralization and durability of 2 or 3 doses of the BNT162b2 vaccine against Omicron SARS-CoV-2. *Cell Host Microbe*. 2022;30(4):485–e4883.
60. Planas D, Saunders N, Maes P, Guivel-Benhassine F, Planchais C, Buchrieser J, Bolland WH, Porrot F, Staropoli I, Lemoine F, Péré H, Veyer D, Puech J, Rodary J, Baele G, Dellicour S, Raymenants J, Gorissen S, Geenen C, Vanmechelen B, Wawina-Bokalanga T, Marti-Carreras J, Cuyppers L, Sève A, Hocqueloux L, Prazuck T, Rey FA, Simon-Loriere E, Bruel T, Mouquet H, André E, Schwartz O. Considerable escape of SARS-CoV-2 Omicron to antibody neutralization. *Nature*. 2022;602(7898):671–5.
61. Schmidt F, Muecksch F, Weisblum Y, Da Silva J, Bednarski E, Cho A, Wang Z, Gaebler C, Caskey M, Nussenzweig MC, Hatziioannou T, Bieniasz PD. Plasma neutralization of the SARS-CoV-2 Omicron variant. *N Engl J Med*. 2022;386(6):599–601.
62. Zhou T, Zhu J, Wu X, Moquin S, Zhang B, Acharya P, Georgiev IS, Altae-Tran HR, Chuang GY, Joyce MG, Kwon YD, Longo NS, Louder MK, Luongo T, McKee K, Schramm CA, Skinner J, Yang Y, Yang Z, Zhang Z, Zheng A, Bonsignori M, Haynes BF, Scheid JF, Nussenzweig MC, Simek M, Burton DR, Koff WC, Mullikin JC, Connors M, Shapiro L, Nabel GJ, Mascola JR, Kwong PD. Multidonor analysis reveals structural elements, genetic determinants, and maturation pathway for HIV-1 neutralization by VRC01-class antibodies. *Immunity*. 2013;39(2):245–58.
63. Ju B, Fan Q, Liu C, Shen S, Wang M, Guo H, Zhou B, Ge X, Zhang Z. Omicron BQ.1.1 and XBB.1 unprecedentedly escape broadly neutralizing antibodies elicited by prototype vaccination. *Cell Rep*. 2023;42(6):112532.
64. Li Y, Fan Q, Zhou B, Shen Y, Zhang Y, Cheng L, Qi F, Song S, Guo Y, Yan R, Ju B, Zhang Z. Structural and functional analysis of an inter-spike bivalent neutralizing antibody against SARS-CoV-2 variants. *iScience*. 2022;25(6):104431.
65. Cheng L, Song S, Fan Q, Shen S, Wang H, Zhou B, Ge X, Ju B, Zhang Z. Cross-neutralization of SARS-CoV-2 Kappa and Delta variants by inactivated vaccine-elicited serum and monoclonal antibodies. *Cell Discov*. 2021;7(1):112.
66. Zhang Q, Ju B, Ge J, Chan JF, Cheng L, Wang R, Huang W, Fang M, Chen P, Zhou B, Song S, Shan S, Yan B, Zhang S, Ge X, Yu J, Zhao J, Wang H, Liu L, Lv Q, Fu L, Shi X, Yuen KY, Liu L, Wang Y, Chen Z, Zhang L, Wang X, Zhang Z. Potent and protective IGHV3-53/3–66 public antibodies and their shared escape mutant on the spike of SARS-CoV-2. *Nat Commun*. 2021;12(1):4210.
67. Guo H, Jiang J, Shen S, Ge X, Fan Q, Zhou B, Cheng L, Ju B, Zhang Z. Additional mutations based on Omicron BA.2.75 mediate its further evasion from broadly neutralizing antibodies. *iScience*. 2023;26(4):106283.
68. Ju B, Zhou B, Song S, Fan Q, Ge X, Wang H, Cheng L, Guo H, Shu D, Liu L, Zhang Z. Potent antibody immunity to SARS-CoV-2 variants elicited by a third dose of inactivated vaccine. *Clin Transl Med* 2022, 12 (2), e732.
69. Ju B, Li D, Ren L, Hou J, Hao Y, Liang H, Wang S, Zhu J, Wei M, Shao Y. Identification of a novel broadly HIV-1-neutralizing antibody from a CRF01_AE-infected Chinese donor. *Emerg Microbes Infect*. 2018;7(1):174.

Publisher's note

Springer Nature remains neutral with regard to jurisdictional claims in published maps and institutional affiliations.